Blowout limit of premixed flame in a micro preheated combustor with a flame holder at different blockage ratios

Jianlong Wan[*], Haibo Zhao

State Key Laboratory of Coal Combustion, School of Energy and Power Engineering, Huazhong University of Science and Technology, Wuhan, 430074, China

HIGHLIGHTS

- Blowout limit is studied at the synergistic effect of heat and flow recirculation.
- Blowout limit first increases and then decreases with increased blockage ratio.
- Heat recirculation and preferential transport effect determine the blowout limit.
- A moderate width of flame holder is more suitable for the present combustor.
- This study provides theoretical basis to optimize the combustor with bluff body

ARTICLE INFO

ABSTRACT

A micro preheated combustor with a flame holder was developed to take full advantage of both heat and flow recirculation. In the present study, the effect of blockage ratio (ξ) on the blowout limit of methane/air premixed flame is investigated. The blockage ratio increases by increasing the width of the flame holder in a combustion chamber with a constant height, while the inflow channel width correspondingly decreases. It is interesting to find that the blowout limit first increases and then decreases with increased ξ. Then, the underlying mechanisms are analyzed in terms of the flow field, stretch effect, heat transfer effect, and preferential transport. The analysis indicates that the direct effect of flow field on the present non-monotonic blowout limit is marginal. A larger stretch effect and heat-loss to the flame holder can induce the decrease in blowout limit from $\xi = 0.6$ to $\xi = 0.7$. The change rules of the heat recirculation and preferential transport effects are consistent with that of the blowout limit. The heat recirculation effect on the fresh mixture and preferential transport effect on the flame root are the best at $\xi = 0.6$, which contributes to the largest blowout limit at $\xi = 0.6$. Thus, a larger width of flame holder does not always guarantee a bigger blow-off limit. The present work not only provides guideline for reasonably choosing the size of the flame holder in the similar micro combustors but also helps us to gain insights into the combustion characteristics under the aforementioned competitive effects.

© 2020 Hydrogen Energy Publications LLC. Published by Elsevier Ltd. All rights reserved.

* *Corresponding author.* State Key Laboratory of Coal Combustion, Huazhong University of Science and Technology, 1037 Luoyu Road, Wuhan, 430074, China.
E-mail addresses: jlw@hust.edu.cn, 648653676@qq.com (J. Wan).

Introduction

As the energy densities of hydrocarbon fuels are much higher than that of conventional electrochemical batteries, the combustion-based miniature power generators which can provide power sources for micro-electro-mechanic systems have attracted extensive attention [1,2]. However, the flames in micro- or meso-scale combustors easily lose stability due to several challenges. The first issue is that the flame quenching near the wall probably occurs owing to the sharply increased heat losses as the surface area-to-volume ratio of the combustor increases dramatically [3]. In addition, the residence time of gaseous mixture in combustion chamber is very short. Due to the adversity under micro-scale, there exist many unstable flame forms, such as oscillating flames [4,5], x-shaped spinning flames [6,7], and spiral flames [8,9]. Thus, it is urgently necessary to develop the micro- or meso-scale combustors with a wide stable and safe operating range.

Various solutions have been adopted to promote micro flame stability. For instance, the heat recirculation method was often applied to broaden the flammable limits of fuel mixture as it can significantly compensate for the heat loss from the meso-scale combustor to the ambient environment. The "Swiss-roll" combustor was a typical configuration which uses the heat recirculation to stabilize micro flames [10,11]. The flammability limit of fuel-oxidizer premixed mixture was significantly extended in the Swiss-roll combustors. The heat recirculation effect of micro combustors with porous media was also remarkable, which obviously improves the flame stabilization [12–14]. Li et al. [12] found that the heat exchange performance between the gaseous mixture and solid matrix played the dominant role in preheating the fresh mixture. Liu et al. [13] demonstrated that heat conduction in the solid wall had a crucial effect on the combustion efficiency of methane-air premixed mixture. However, the flame cannot be effectively anchored, which narrows the flame blowout limits in these combustors.

To form flow recirculation via structural design (such as wall cavity and bluff-body) was an effective way to anchor micro flames [15–20]. Yang et al. [17] found that the backward facing step could remarkably prolong the residence time of gaseous mixture in a tube combustor and anchor the flame location. Peng et al. [21] pointed out that the flow recirculation zone behind the backward-facing step effectively improved the stabilization of hydrogen/air premixed flames in the micro tube-combustor. The backward-facing step could also increase the wall temperature level of the micro tube-combustor [22]. Wan et al. [23–26] and Li et al. [27] investigated the combustion characteristics of premixed hydrogen/air and methane/air in micro- or mesoscale combustor with wall cavities, and results showed that the cavity has a good ability to anchor the flame. As a result, the flame blow-off limits of methane-air premixed mixture and the combustion efficiency of hydrogen-air premixed mixture in these combustors were significantly enlarged. Moreover, Wan et al. [28,29] also developed a micro combustor with a triangle bluff-body which can expand the blow-off limit of hydrogen/air premixed flame by several times compared to that using the straight channel. Yan et al. [30] found that the blow-off limit of

micro hydrogen/air premixed flame can be remarkably enlarged by a triangular bluff-body with two side slits. The blow-off limit of methane/air premixed flame could also be significantly enlarged in the micro bluff-body combustor [31,32]. In addition, the bluff-body could obviously improve the thermal and emission performances of the micro combustor [33,34]. Zhang et al. [35] found that the combustion efficiency of hydrogen-air premixed mixture in a micro combustor with wall cavities and a bluff-body was higher than that in a micro combustor only with wall cavities. These papers indicate that the flame can be well anchored by the flow recirculation zone in the combustion chamber, but the flammable limits of fuel-oxidizer mixture in these combustors are not wide.

In order to jointly utilize the advantages of heat and flow recirculation, we developed a micro preheated combustor with a flame holder in our previous publications [36,37], and the results showed that the premixed flame stabilization of lean methane/air can be significantly improved in the combustor [36,37]. The numerical results showed that the copper combustor had a widest operational range while the SiC combustor had the poorest performance. To obtain a large flame blow-off limit, a solid material with a large thermal conductivity and a small emissivity was suggested to fabricate this kind of micro combustor [36]. The blowout limit of methane-air premixed flame first increased and then decreased with an increasing length of the flame holder [37]. The present study investigates the effect of the blockage ratio on the flame blowout limit in this micro combustor, which can provide the guideline for further optimizing the present combustor. In addition, the present study can help us to better understand the micro combustion characteristics under the synergistic effect of heat and flow recirculation which widely exists in the practical combustors. Therefore, the present study also provides a guideline to optimize other practical combustors.

Numerical methods

Geometric model of the combustor

Fig. 1 schematically shows the geometric structure of the preheated two-dimensional combustor with a flame holder. For the sake of a clear discussion, the whole flow channel is divided into the preheating channels and combustion chamber by the yellow solid lines. The wall thickness (δ) of the combustor is 0.5 mm. The height of the combustion chamber maintains at 2.0 mm. The widths of the flame holders (H) are 0.8, 1.0, 1.2, and 1.4 mm, respectively, and the corresponding blockage ratios (H/2.0 mm) are 0.4, 0.5, 0.6, and 0.7, respectively. In addition, the length of the flame holder is 6.0 mm. Other geometrical dimensions are presented in Fig. 1.

Mathematical model

The calculated results show that the present magnitude of Knudsen number is 10^{-5}, which is much smaller than the critical value (0.001). Therefore, the gaseous mixture can be reasonably regarded as a continuum and the Navier-Stokes
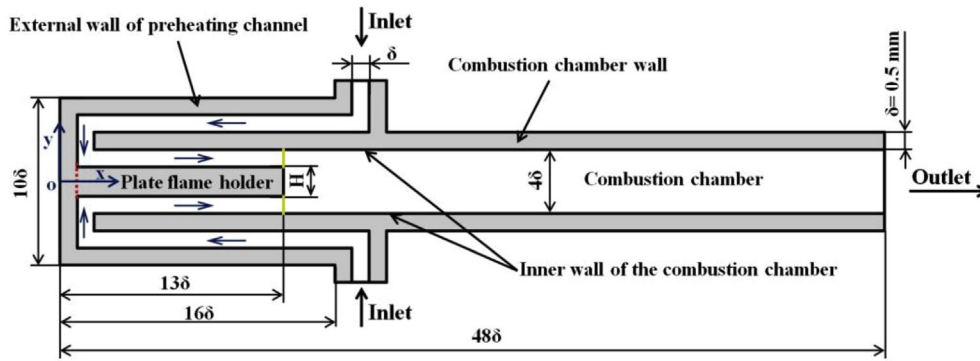
Fig. 1 — Schematic of the present two-dimensional combustor.

equations are applicable for the present study [38]. The largest Reynolds number of the cold fuel mixture is ~400, and a steady-state laminar flow model was used in the present and previous computations [36,37], which is able to directly solve the conservation equations. Governing equations can be obtained from our previous publication [36]. The Second Order Upwind was employed to discrete space in the current numerical simulation.

Computation scheme

The ANSYS Fluent 14.5 [39] was employed to solve the mass, momentum, energy, and species conservation equations, with the detailed thermodynamic and transport properties from the CHEMKIN databases [40] and the C1 reaction mechanism which includes 18 species and 58 reactions [41]. Table 1 lists the initial parameters and boundary conditions for the numerical simulation.

The heat loss from the combustor to the ambient environment $q = h_s(T_{W,O} - T_\infty) + \varepsilon_s\sigma(T_{W,O}^4 - T_\infty^4)$: $h_s = 20\,\mathrm{W\,m^{-2}\,K^{-1}}$ (the heat transfer coefficient of natural convection) [42]; $T_{w,o}$ is the outer wall temperature of the combustor, $T_\infty = 300$ K (the ambient temperature); $\varepsilon_s = 0.2$ (the emissivity of the outer wall surface) [43]; $\sigma = 5.67 \times 10^{-8}\,\mathrm{W\,m^{-2}\,K^{-4}}$ (the Stephan-Boltzmann constant).

Same as before, in order to reasonably reduce the computation load, half of the configuration was employed [36,37]. Grid independency has been checked by using three sets of grid system, as shown in Fig. 2. The results obtained by these three grid systems are almost overlapped with each other, which indicates that the flame structure can be well captured using the grid size of 50 μm. Further refinement of the meshes

(the minimum grid size is 25 μm) near the flame holder was conducted, i.e., a nonuniform grid system was employed. This strategy was also adopted in our previous study [36,37]. The convergence criteria for the residuals of the computational results were smaller than 1.0×10^{-6}. It should be pointed out that the same numerical models and methods were also adopted to simulate the methane/air combustion characteristics in a similar mesoscale combustor in our previous work, and the numerical results generally agree with the experimental data reasonably well [44]. Therefore, it is believed that the present numerical model/method is reasonable. As a result, the current numerical results are solid. It should be pointed out that our previous publications [23,28] and Li et al. [12] indicated that the effect of the side walls on the combustion characteristics can be nearly ignored when the ratio between the width and height of the micro combustion chamber is bigger than 10.0 through quantitatively comparing the experimental and numerical results. Therefore, we think that the present analyses are tenable when the width of the present combustor is larger than 20.0 (2.0 × 10) mm.

Results and discussions

Blowout limits with different blockage ratios

The flame blowout limit is defined as the critical inlet velocity V_{in} (i.e., the largest V_{in}) over which the flame is blown out of the combustion chamber and then extinguished. Fig. 3 shows the blowout limits of lean methane/air premixed flame in the combustor with different blockage ratios. This figure demonstrates that, with the co-existence of the flame holder and

| Table 1 — Initial parameters and boundary conditions for the present numerical simulation.	
Item	Setting
Fuel	Methane
Oxidizer	Air
Solid material	Stainless steel with a thermal conductivity of 24 W/(m·K) [36]
Inlet	Uniform concentration and velocity distributions at 300 K
Outlet	Neumann boundary
Interface between the fluid and solid	"Coupled" method
Inner wall	Chemically inert with no slip
Heat loss from the outer wall to the environment	Including the natural convection and radiation-heat losses [36]
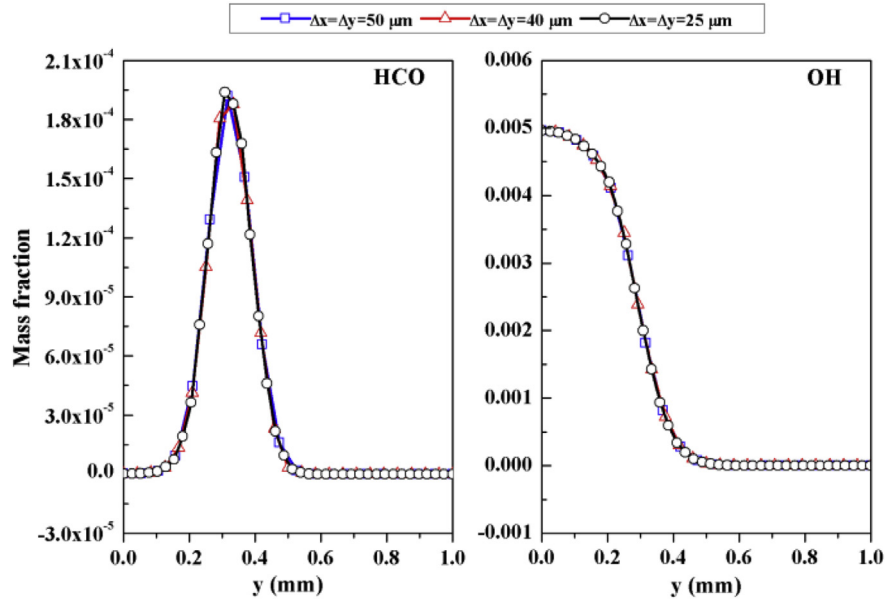
Fig. 2 — Mass fraction profiles of HCO and OH near the flame front ($x = 8.0$ mm) in the vertical direction (0 mm $\leq y \leq$ 1 mm) for three different grid resolutions at $\phi = 0.7$ and $V_{in} = 3.0$ m/s.
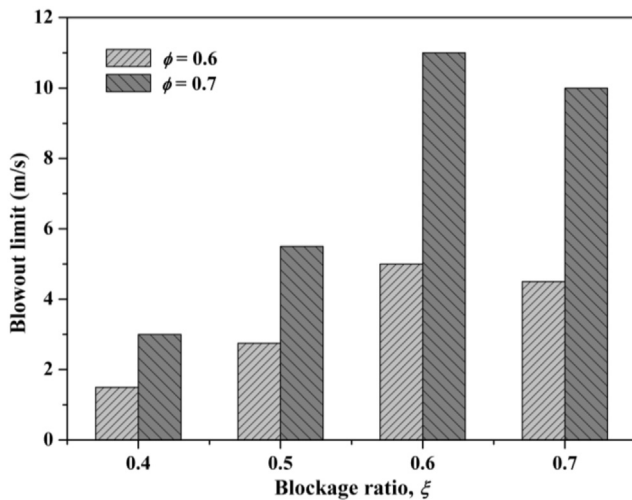

Fig. 3 — Flame blowout limits for various blockage ratios at $\phi = 0.6$ and 0.7.

preheating channels, a large blowout limit is achieved for lean fuel mixtures ($\phi = 0.6$ and 0.7) even if the height of combustion chamber (2.0 mm) is narrower than the quenching distance of stoichiometric methane/air premixed fuel mixture at the ambient temperature and pressure (~2.5 mm). For example, the blowout limits at $\phi = 0.6$ for $\xi = 0.4$, 0.5, 0.6, and 0.7 are 1.5 m/s, 2.75 m/s, 5.0 m/s, and 4.5 m/s, respectively. More importantly, the blowout limit first increases and then decreases with increased blockage ratio, i.e., a non-monotonic function relation. In the micro combustor with a bluff body [45], the blowout limit increases with increasing blockage ratios, which is significantly different from the present variation law. This is probably because, for the cases with the bluff body, the positive effect brought by the increase of blockage ratio (an increased recirculation zone) plays the main role in

determining the blowout limit. However, for the cases with the co-existence of flame holder and preheating channels, the weight of each competing factor which influences the flame stabilization changes, which results in a non-monotonic blowout limit. For example, for the present cases, the increase in blockage ratio not only enlarges the recirculation zone behind the flame holder but also increases the flow velocity and decreases the residence time of fresh mixture in the preheating channel, which makes the heat recirculation effect on the fresh mixture complicated. Moreover, on one hand, the increase in blockage ratio can directly affect the flow two-dimensionality effect around the flame holder, which significantly influences the preferential transport effect; on the other hand, the mass diffusion coefficient of reactive species has a different sensitivity to changes in temperature (for example, the increasing rates of H_2 and H diffusion velocities (the fast-diffusing species) are larger with increased temperature), so the preferential transport effect can be indirectly influenced by the increased blockage ratio via the heat recirculation effect. It can be seen that the combustion characteristics under the synergistic effect of heat and flow recirculation are complicated. The present interesting results may be a new feature in the micro combustor with the aforementioned synergistic effect, which has never been reported before. Next, the underlying mechanisms will be detailed in terms of the flow field, stretch effect, heat transfer effect, and preferential transport effect [46].

Mechanisms of non-monotonic blowout limit

Three neighboring cases ($\xi = 0.5$, 0.6, and 0.7) are adopted to reveal the underlying mechanisms responsible for the present non-monotonic blowout limit. For the convenience of a quantitative discussion, the flame front is defined. Similar to our previous publications [36,37,47], we use the normalized isoline corresponding to 15% of maximum mass fraction of

HCO (Y_{HCO}) to visualize flame front in this study. Same as before [20,44], the flame front near the flame holder (upstream part) and near the combustion chamber wall (downstream part) are defined as the flame root and flame top, respectively.

Flow field

The flow field in the present combustion chamber mainly has two direct effects on the flame stabilization: the recirculation zone (RZ) generated behind the flame holder is beneficial for the flame stabilization (the positive effect); the incoming flow directly pushes the flame front out of the RZ downstream (the negative effect). Fig. 4 shows the flow field with overlaid flame front at different blockage ratios. Generally, a larger RZ is helpful for improving the flame root stabilization due to the larger counter flow which can prevent the flame root from being pushed downstream. Fig. 4 shows that, with the increased blockage ratio, the RZ area increases (the heights of RZ at ξ = 0.5, 0.6 and 0.7 are 0.77 mm, 1.06 mm and 1.48 mm, respectively), but the area of the flame root within the recirculation zone (*i.e.*, the area of the flame front in the flow velocity isoline of 0.0 m/s) decreases, which is slightly detrimental for the flame root stabilization. This is because
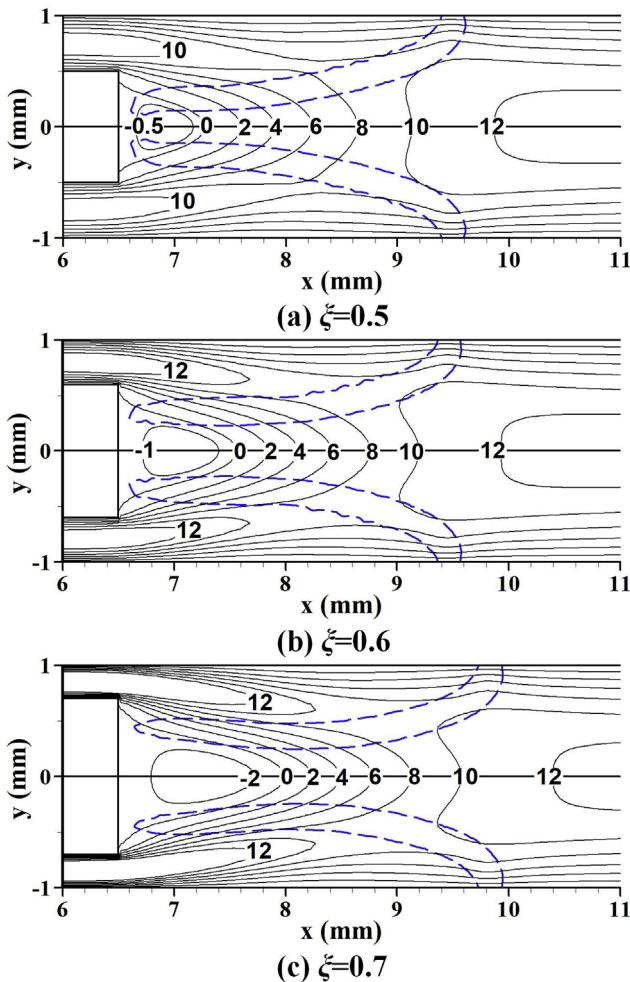
the increased blockage ratio leads to a decreasing flow area between the flame holder and combustion chamber wall. As a result, the flow velocity around the inlet of combustion chamber is larger, which significantly influences the flame shape, as shown in Fig. 4.

In order to observe the negative effect of flow field on the flame stabilization, we present the acute angle profiles between the acute angle between the normal direction of the flame front and flow direction (θ_n), the local flow velocity (V_{local}), and the local flow velocity in the direction perpendicular to the flame front (V_n) around the middle of flame front for different blockage ratios in Fig. 5. It should be pointed out that the $V_n = V_{local} \times \cos \theta_n$. It can be seen that V_{local} first increases and then decreases along the flame front towards downstream, which is the conventional structure of flow filed for the cases with the sudden expansion of flow channel width. In addition, the θ_n increases with increased ξ. As the comprehensive result of θ_n and V_{local}, V_n almost increases along the flame front towards downstream for each ξ. More importantly, V_n first increases and then decreases with increased ξ, *i.e.*, V_n at ξ = 0.6 is the largest among them. As we know, $|S| = |V_n|$ (the flame speed (S) is equal to the V_n) is the necessary condition for the stable flame. If $|V_n|$ is larger than $|S|$, the flame will shift downstream along the normal direction of flame front towards the combustion products. Thus, under the same equivalence ratio, pressure, and temperature of the fresh mixture, a larger V_n is detrimental to the flame stabilization. Therefore, we speculate that the direct effect of flow field on the present non-monotonic blowout limit is marginal.

Stretch effect

It is known that the flame stabilization is influenced by the stretch effect, and a larger stretch rate is detrimental for the flame stabilization out of RZ. Therefore, we should quantitatively obtain the stretch rate (k) along the flame front out of RZ. As we know, $k = k_c + k_s$: k_c and k_s are the curvature and strain rates, respectively [46]. For the present flat flame, the contribution of k_c to k can be neglected [48,49], *i.e.*, $k \approx k_s$. The strain rate (k_s) can be obtained by the following Eq. (1) [48]:

$$k_s - n_x n_y \left(\frac{\partial u}{\partial y} + \frac{\partial v}{\partial x} \right) - n_x^2 \frac{\partial u}{\partial x} - n_y^2 \frac{\partial v}{\partial y} \tag{1}$$

where $-n_x n_y \left(\frac{\partial u}{\partial y} + \frac{\partial v}{\partial x} \right) = k_{s,s}$ (the contribution of the shear); $-n_x^2 \frac{\partial u}{\partial x} - n_y^2 \frac{\partial v}{\partial y} = k_{s,n}$ (the contribution of the normal strain); n is the normal direction of the flame front.

Fig. 6 presents the distribution characteristics of $k_{s,s}$, $k_{s,n}$ and k_s along the upstream boundary of flame front towards downstream for different blockage ratios. Fig. 6a shows that $k_{s,s}$ is almost equal to $k_{s,n}$, *i.e.*, $k_{s,s}$ and $k_{s,n}$ have the same contribution for k_s, which is significantly different from the component characteristic of k_s which is determined by the $k_{s,n}$ in the similar mesoscale combustor [48]. Fig. 6b presents that the k_s increases with an increased blockage ratio (a monotonous variation law), and the amplitude is increasing, which has a negative effect on the flame stabilization in the combustion chamber. Therefore, a larger stretch effect can induce the decrease in blowout limit from ξ = 0.6 to ξ = 0.7.
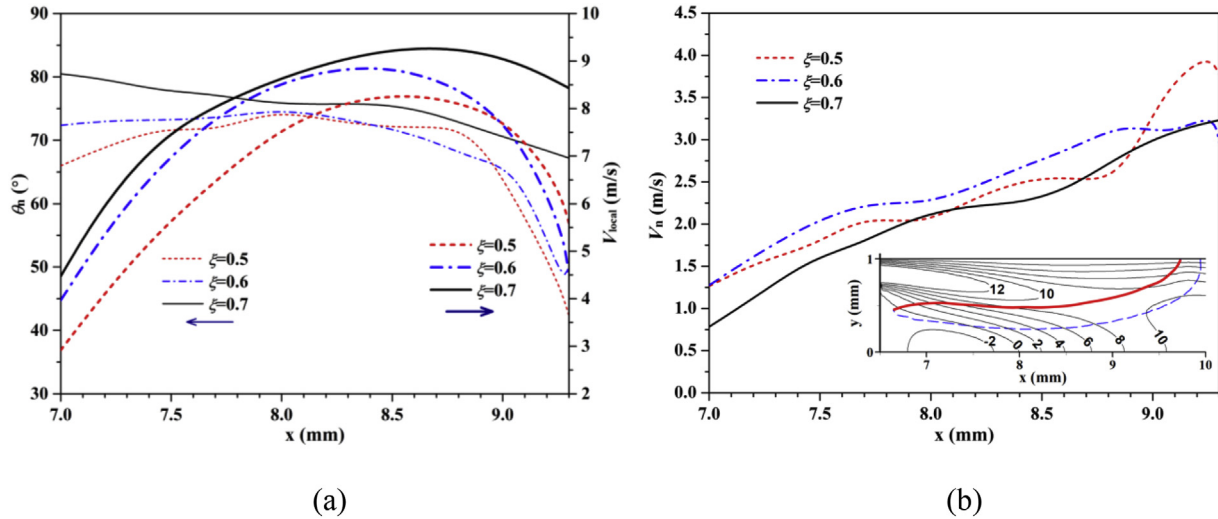

Fig. 4 – **Flow field with overlaid flame front (15% maximum Y_{HCO} isoline) for various blockage ratios at V_{in} = 3.0 m/s and ϕ = 0.7.**

Fig. 5 – The acute angle between the normal direction of the flame front and flow direction (θ_n), and the local flow velocity (V_{local}) (a); the local flow velocity in the direction perpendicular to the flame front (V_n) along the upstream boundary of flame front (the red solid line in the insert) around the middle of flame front (7.0 mm $\leq x \leq$ 9.3 mm) for various blockage ratios at V_{in} = 3.0 m/s and ϕ = 0.7. (For interpretation of the references to color in this figure legend, the reader is referred to the Web version of this article.)
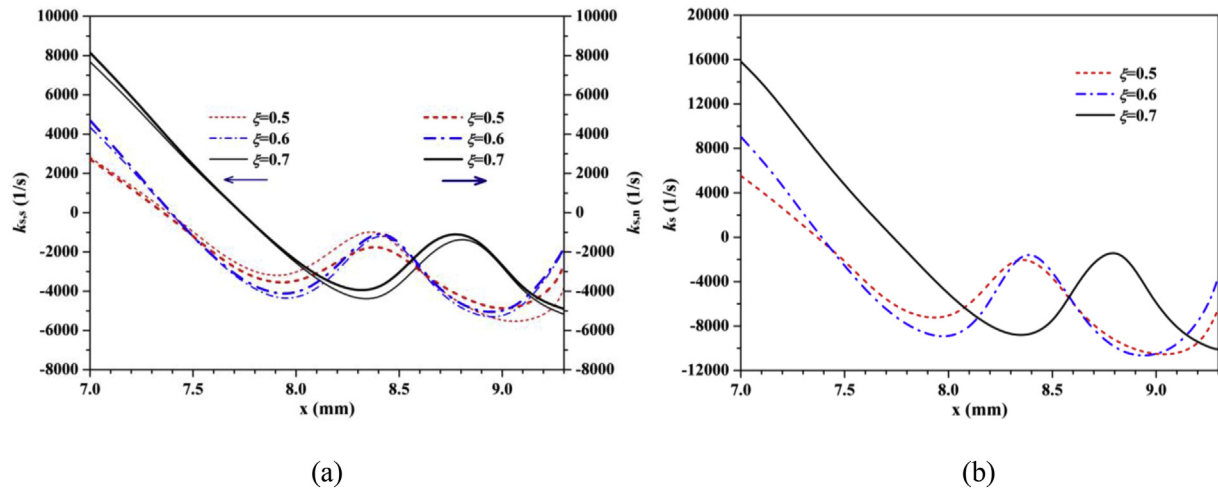

Fig. 6 – $k_{s,s}$, $k_{s,n}$ (a) and k_s (b) profiles along the upstream boundary of flame front towards downstream for various blockage ratios at V_{in} = 3.0 m/s and ϕ = 0.7.

Heat transfer effect

As we know, the flame stabilization is remarkably influenced by the heat transfer effect of the solid walls [50]. On one hand, the heat loss from the flame to the solid walls is detrimental for the flame stabilization (the negative effect); on the other hand, the heat recirculation effect of solid walls which can significantly improve the fresh mixture temperature is beneficial for the flame stabilization (the positive effect). As the standoff distances between the flame root and flame holder are very short in the present cases, the heat-loss from the flame to the flame holder is remarkable, which has negative effect on flame stabilization. Fig. 7a shows that the heat flux that enters the downstream flame holder wall (the heat-loss for the flame) significantly increases with increased ξ, and

the average heat flux at ξ = 0.5, 0.6 and 0.7 are −204224, −234,636 and −252,287 W/m², respectively. Moreover, it should be pointed out that the surface area of the end wall of flame holder also increases. Therefore, the heat-loss from the flame root to the holder significantly increases with increased ξ. Fig. 7b quantitatively shows the heat-loss amount from the flame root to the flame holder at various blockage ratios. It can be seen that the heat-loss ratio nearly increase with the increase in ξ. This is detrimental for the flame root stabilization.

Subsequently, the heat recirculation effect of solid walls on the fuel mixture (i.e., the preheated effect on the fuel mixture) is also investigated. Fig. 8a shows the fresh mixture temperature at the inlet of combustion chamber. It is obtained that the average gas temperature at ξ = 0.5, 0.6 and 0.7 are 827.1 K,
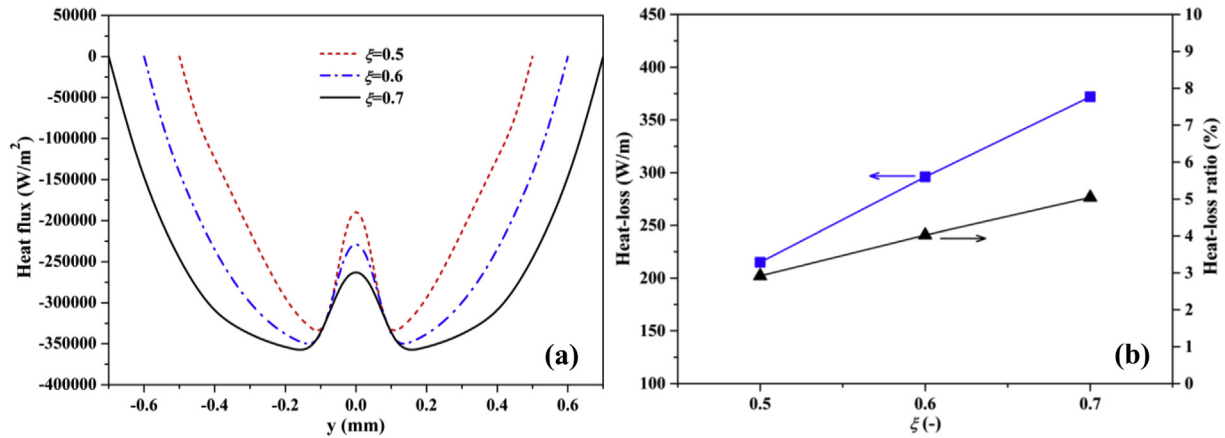
Fig. 7 − The heat flux profiles entering the flame holder (the heat loss for the flame root) (a) and the heat-loss ratio from the flame to the flame holder (b) for various blockage ratios at $V_{in} = 3.0$ m/s and $\phi = 0.7$.

834.9 K and 834.5 K, respectively. In other words, the preheating temperature of fresh mixture at $\xi = 0.6$ is the highest. This is a comprehensive result of the following two factors. On the one hand, the larger heat flux entering the flame holder at a bigger ξ results in a higher end-wall temperature of flame holder, and the increasing amplitude of end-wall temperature is larger from $\xi = 0.5$ to 0.6 (see Fig. 8b). However, the inner surface temperature of combustion chamber wall in the preheating channel decreases with increased ξ. The decreased amplitude is smaller from $\xi = 0.5$ to 0.6. Therefore, the temperature of preheating wall at $\xi = 0.6$ is higher. On the other hand, the increase in ξ reduces the width of preheating channel around the inlet of combustion chamber, which results in two competitive effects: the residence time of fuel

mixture in the preheating channel decreases due to a faster flow velocity (the negative effect), which is detrimental for the heat exchange between the high temperature wall and the fresh mixture of low temperature; the heat transfer coefficient between the wall surface and fresh mixture increases to some extent (the positive effect), which is beneficial for the heat exchange between them. Therefore, it is deduced that a better heat recirculation effect (including a higher temperature of preheating wall, a longer residence time of fresh mixture and a larger heat transfer coefficient between the wall surface and fresh mixture) results in a higher preheating temperature of fresh mixture at $\xi = 0.6$, which is consistent with the non-monotonic change rule of blowout limit.
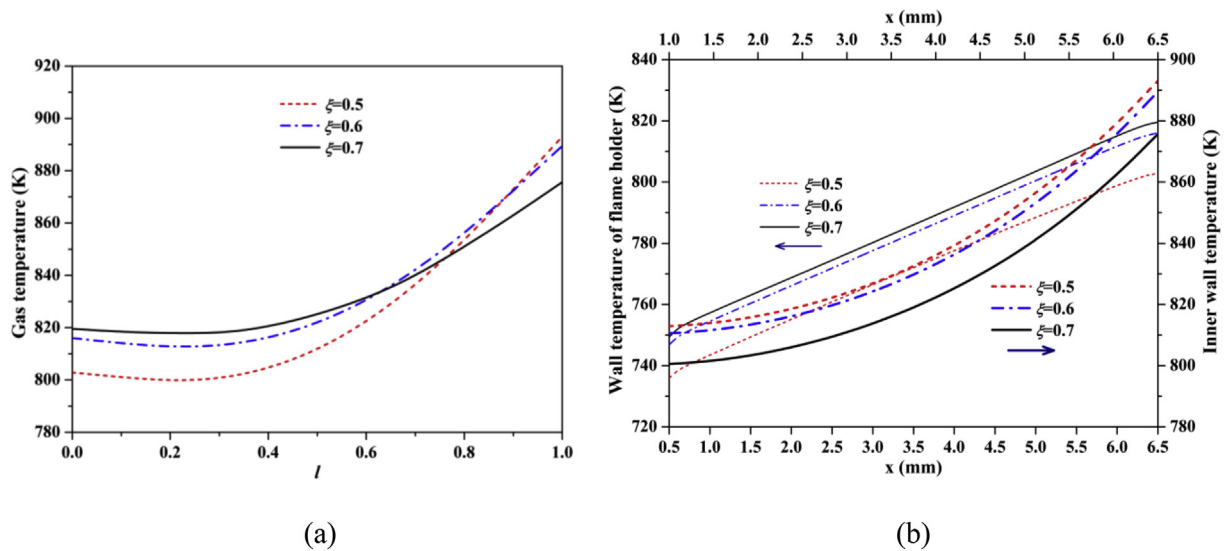

(a)   (b)

Fig. 8 − Gas temperature profiles at the inlet of combustion chamber ($x = 6.5$ mm, l is the dimensionless height of combustion chamber inlet, $l=(l_y − l_{fh})/l_{cci}$: l_y is the y-coordinate of each point at the combustion chamber inlet; l_{fh} is the half height of flame holder; l_{cci} is the height of combustion chamber inlet) (a); the temperature profiles of horizontal wall of flame holder ($y = 0.5$ mm, 0.5 mm $\leq x \leq 6.5$ mm) and inner surface of combustion chamber wall ($y = 1.0$ mm, 1.0 mm $\leq x \leq 6.5$ mm) (b) for various blockage ratios at $V_{in} = 3.0$ m/s and $\phi = 0.7$.
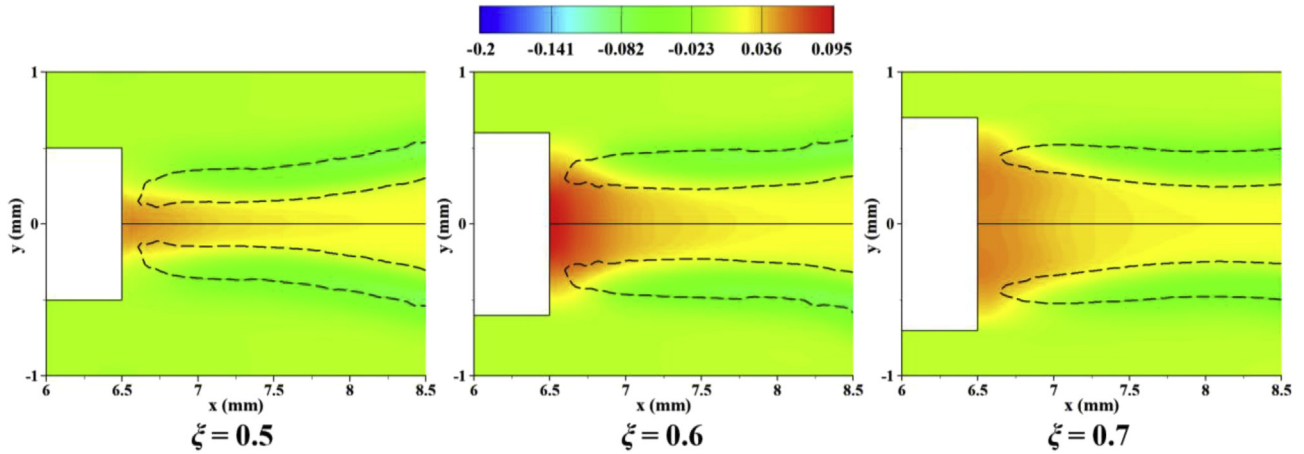
Fig. 9 – Colored contours of ϕ_{local}-ϕ with overlaid flame front near the flame root for various blockage ratios.
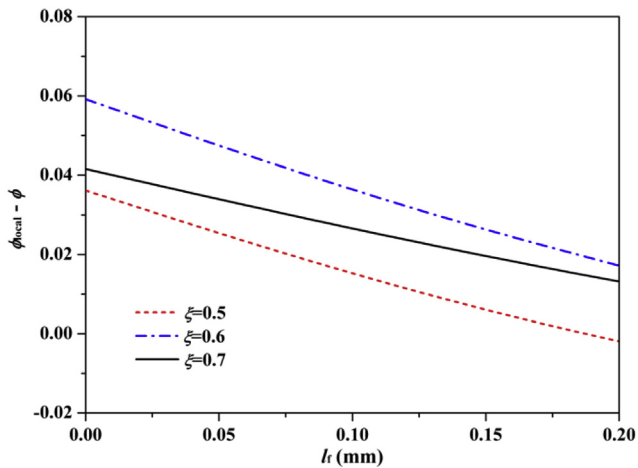

Fig. 10 – ϕ_{local}-ϕ profiles along the upstream boundary of flame front from the flame root towards downstream for various blockage ratios at $V_{in} = 3.0$ m/s and $\phi = 0.7$.

Based on the aforementioned results and discussion, we can conclude that the heat recirculation effect rather than the heat-loss from the flame root to the flame holder is one factor to determine the present non-monotonic blowout limit, but a larger heat-loss can induce a decrease in the blowout limit from $\xi = 0.6$ to 0.7.

Preferential transport effect
Generally, the preferential transport effect is obvious in the combustor with a bluff-body because the flow two-dimensionality effect is significant, which can increase the local equivalence ratio ϕ_{local} behind the bluff-body [51]. Thus, the preferential transport effect is beneficial for the flame stabilization behind the bluff-body [51–53]. Barlow et al. [51] quantitatively defined ϕ_{local} to evaluate this effect, as presented in Eq. (2):

$$\phi_{local} = \frac{0.5\left(X_{H_2} + X_{H_2O}\right) + X_{CO_2} + X_{CO} + 2X_{CH_4}}{0.5\left(X_{CO} + X_{H_2O}\right) + X_{O_2} + X_{CO_2}} \tag{2}$$

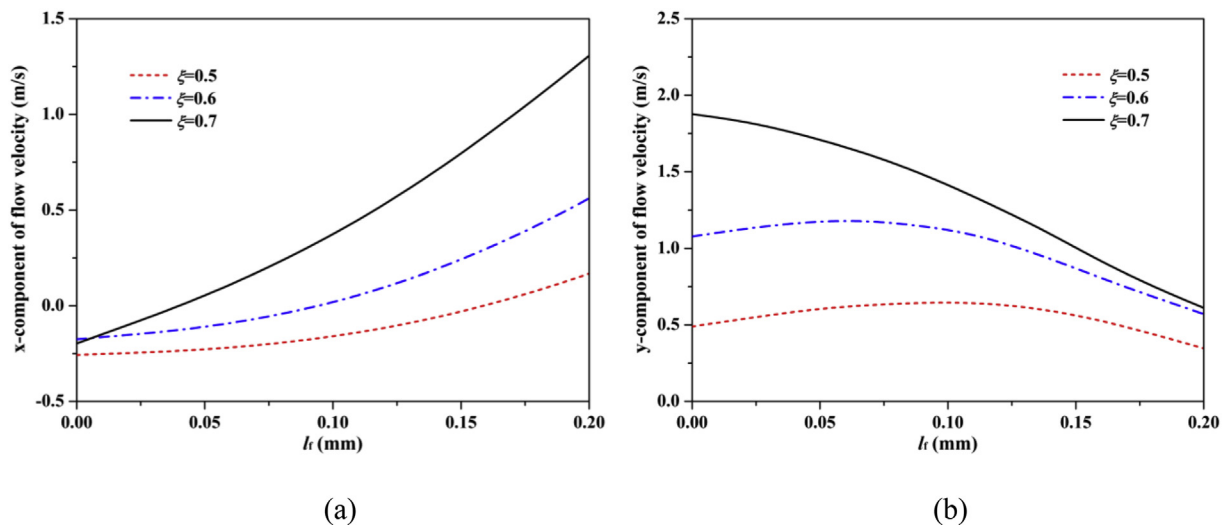where X_i is the mole fraction of species i.

(a)

(b)

Fig. 11 – The profiles of x-component (a) and y-component (b) of flow velocity along the upstream boundary of flame front from the flame root towards downstream for various blockage ratios at $V_{in} = 3.0$ m/s and $\phi = 0.7$.

At first, we observe the distribution characteristics of ϕ_{local} around the flame front in the combustion chamber, as presented in Fig. 9. It can be seen that the high concentration zone of ϕ_{local} for each blockage ratio is just behind the flame holder, and the maximum of ϕ_{local} at $\xi = 0.6$ is the largest although the area of high ϕ_{local} is increasing with increased ξ. Fig. 10 quantitatively shows the distribution characteristics of ϕ_{local}-ϕ (departure from the incoming equivalence ratio) along with the upstream boundary of flame front for different blockage ratios. It can be clearly seen that ϕ_{local} near the flame root at $\xi = 0.6$ is the largest among of them, and it is obtained that ϕ_{local} at the flame root for $\xi = 0.5$, 0.6 and 0.7 are 0.736, 0.759 and 0.742, respectively, which means that the combustion condition at the flame root for $\xi = 0.6$ is the best. This is consistent with the variation law of blowout limit, which indicates that the preferential transport effect is one factor to determine the present non-monotonic blowout limit.

In order to reveal the mechanisms of the aforementioned non-monotonic distribution characteristics of ϕ_{local}, we display the x-component and y-component distribution characteristics of flow velocity along the upstream boundary of flame front in Fig. 11. Fig. 11a shows that the x-component of flow velocity increases more sharply for a larger ξ, which means a larger velocity gradient. As a result, a more significant flow two-dimensionality effect enhances the preferential transport effect, so more flammable species can enter the downstream zone of flame front via diffusion, which contributes to a higher ϕ_{local}. Furthermore, Fig. 11b presents the y-component distribution characteristic of flow velocity which has a more remarkable effect on the mass diffusion velocities of species toward downstream. It can be seen that the y-component of flow velocity is larger for a bigger ξ, and the y-components of flow velocity are positive values. This means that the flow direction of y-component is towards the reactants, which prevents that the flammable species enter the downstream zone of flame front via convective transport. Therefore, a larger y-component of flow velocity is detrimental for improving ϕ_{local}. These two competitive effects make ϕ_{local} reach the optimal value at $\xi = 0.6$.

Conclusions

The present study mainly studies the effect of blockage ratio on the blowout limit of methane/air premixed flame in a micro preheated combustor with a flame holder. The blockage ratio increases by increasing the width of the flame holder in a combustion chamber with a constant height, while the inflow channel width correspondingly decreases. A non-monotonic blowout limits are unexpectedly found. Specifically, the blowout limit first increases and then decreases with increased blockage ratio ξ. Then, the underlying mechanisms are analyzed in detail. It is found that the direct effect of flow field on the present non-monotonic blowout limit is marginal. A larger stretch effect and heat loss can induce the decrease in blowout limit from $\xi = 0.6$ to $\xi = 0.7$. The change rules of the heat recirculation and preferential

transport effects varying ξ are consistent with that of the blowout limit. The best heat recirculation effect on the fresh mixture and preferential transport effect on the flame root contribute to the largest blowout limit at $\xi = 0.6$. Therefore, a larger width of flame holder does not always guarantee a better flame stabilization. This indicates that the weight of each competing factor which influences the flame stabilization may change under the synergistic effect of heat and flow recirculation which exists in many practical micro combustors. Therefore, it is necessary to systematically study the flame dynamics under the aforesaid synergistic effect, which will be investigated in our next work.

Declaration of competing interest

The authors declare that they have no known competing financial interests or personal relationships that could have appeared to influence the work reported in this paper.

Acknowledgements

REFERENCES

[1] Ju Y, Maruta K. Microscale combustion: technology development and fundamental research. Prog Energy Combust Sci 2011;37:669—715.
[2] Maruta K. Micro and mesoscale combustion. Proc Combust Inst 2011;33:125—50.
[3] Leach TT, Cadou CP. The role of structural heat exchange and heat loss in the design of efficient silicon micro-combustors. Proc Combust Inst 2005;30:2437—44.
[4] Pizza G, Frouzakis CE, Mantzaras J, Tomboulides AG, Boulouchos K. Dynamics of premixed hydrogen/air flames in microchannels. Combust Flame 2008;152:433—50.
[5] Xiang Y, Zhao M, Huang H, Fan A. Experimental investigation on the scale effects on diffusion H2/air flames in Y-shaped micro-combustors. Int J Hydrogen Energy 2019;44:30462—71.
[6] Xu B, Ju Y. Experimental study of spinning combustion in a mesoscale divergent channel. Proc Combust Inst 2007;31:3285—92.
[7] Wan JL, Shang C, Zhao H. Dynamics of methane/air premixed flame in a mesoscale diverging combustor with/without a cylindrical flame holder. Fuel 2018;232:659—65.
[8] Fan AW, Wan JL, Maruta K, Nakamura H, Yao H, Liu W. Flame dynamics in a heated meso-scale radial channel. Proc Combust Inst 2013;34:3351—9.
[9] Kumar S, Maruta K, Minaev S. On the formation of multiple rotating Pelton-like flame structures in radial microchannels with lean methane—air mixtures. Proc Combust Inst 2007;31:3261—8.
[10] Kim N, Kato S, Kataoka T, Yokomori T, Maruyama S, Fujimori T, et al. Flame stabilization and emission of small

Swiss-roll combustors as heaters. Combust Flame 2005;141:229–40.

[11] Kuo CH, Ronney PD. Numerical modeling of non-adiabatic heat-recirculating combustors. Proc Combust Inst 2007;31:3277–84.

[12] Li J, Li Q, Shi J, Liu X, Guo Z. Numerical study on heat recirculation in a porous micro-combustor. Combust Flame 2016;171:152–61.

[13] Liu Y, Fan A, Yao H, Liu W. Numerical investigation of filtration gas combustion in a mesoscale combustor filled with inert fibrous porous medium. Int J Heat Mass Tran 2015;91:18–26.

[14] Bani S, Pan J, Tang A, Lu Q, Zhang Y. Numerical investigation of key parameters of the porous media combustion based Micro-Thermophotovoltaic system. At Energ 2018;157:969–78.

[15] Shanbhogue SJ, Husain S, Lieuwen T. Lean blowoff of bluff body stabilized flames: scaling and dynamics. Prog Energy Combust Sci 2009;35:98–120.

[16] Ansari M, Amani E. Micro-combustor performance enhancement using a novel combined baffle-bluff configuration. Chem Eng Sci 2018;175:243–56.

[17] Yang WM, Chou SK, Shu C, Li ZW, Xue H. Combustion in micro-cylindrical combustors with and without a backward facing step. Appl Therm Eng 2002;22:1777–87.

[18] Wan JL, Zhao H. Effect of conjugate heat exchange of flame holder on laminar premixed flame stabilization in a meso-scale diverging combustor. At Energ 2020;198:117294.

[19] Wan JL, Zhao H. Experimental study on blow-off limit of a preheated and flame holder-stabilized laminar premixed flame. Chem Eng Sci 2020;223:115754.

[20] Wan JL, Wu Y, Zhao H. Excess enthalpy combustion of methane-air in a novel micro non-premixed combustor with a flame holder and preheating channels. Fuel 2020;271:117518.

[21] Peng Q, Jiaqiang E, Yang WM, Xu H, Chen J, Zhang F, et al. Experimental and numerical investigation of a micro-thermophotovoltaic system with different backward-facing steps and wall thicknesses. At Energ 2019;173:540–7.

[22] Ni S, Zhao D, Sun Y, Jiaqiang E. Numerical and entropy studies of hydrogen-fuelled micro-combustors with different geometric shaped ribs. Int J Hydrogen Energy 2019;44:7692–705.

[23] Wan JL, Yang W, Fan AW, Liu Y, Yao H, Liu W, et al. A numerical investigation on combustion characteristics of H_2/air mixture in a micro-combustor with wall cavities. Int J Hydrogen Energy 2014;39:8138–45.

[24] Wan JL, Fan AW, Yao H, Liu Y, Gou XL, Zhao DQ. The impact of channel gap distance on flame splitting limit of H2/air mixture in microchannels with wall cavities. Int J Hydrogen Energy 2014;29:11308–15.

[25] Wan JL, Fan AW, Liu Y, Yao H, Liu W, Gou XL, et al. Experimental investigation and numerical analysis on flame stabilization of CH4/air mixture in a mesoscale channel with wall cavities. Combust Flame 2015;162:1035–45.

[26] Wan JL, Fan AW. Effect of channel gap distance on the flame blow-off limit in mesoscale channels with cavities for premixed CH4/air flames. Chem Eng Sci 2015;132:99–107.

[27] Li L, Yang W, Fan A. Effect of the cavity aft ramp angle on combustion efficiency of lean hydrogen/air flames in a micro cavity-combustor. Int J Hydrogen Energy 2019;44:5623–32.

[28] Wan JL, Fan AW, Maruta K, Yao H, Liu W. Experimental and numerical investigation on combustion characteristics of premixed hydrogen/air flame in a micro-combustor with a bluff body. Int J Hydrogen Energy 2012;37:19190–7.

[29] Fan AW, Wan JL, Maruta K, Yao H, Liu W. Interactions between heat transfer, flow field and flame stabilization in a micro-combustor with a bluff body. Int J Heat Mass Tran 2013;66:72–9.

[30] Yan Y, Xu F, Xu Q, Zhang L, Yang Z, Ran J. Influence of controllable slit width and angle of controllable flow on hydrogen/air premixed combustion characteristics in micro combustor with both sides–slitted bluff body. Int J Hydrogen Energy 2019;44:20482–92.

[31] Yan Y, Yan H, Zhang L, Li L, Zhu J, Zhang Z. Numerical investigation on combustion characteristics of methane/air in a micro-combustor with a regular triangular pyramid bluff body. Int J Hydrogen Energy 2018;43:7581–90.

[32] Pan J, Zhang C, Pan Z, Wu D, Zhu Y, Lu Q, et al. Investigation on the effect of bluff body ball on the combustion characteristics for methane/oxygen in micro combustor. At Energ 2020;190:116465.

[33] Pan J, Zhu J, Liu Q, Zhu Y, Tang A, Lu Q. Effect of micro-pin-fin arrays on the heat transfer and combustion characteristics in the micro-combustor. Int J Hydrogen Energy 2017;42:23207–17.

[34] Yilmaz H. Investigation of combustion and emission performance of a micro combustor: effects of bluff body insertion and oxygen enriched combustion conditions. Int J Hydrogen Energy 2019;44:25985–99.

[35] Zhang Z, Wu K, Yuen R, Yao W, Wang J. Numerical investigation on the performance of bluff body augmented micro cavity-combustor. Int J Hydrogen Energy 2020;45:4932–45.

[36] Wan JL, Fan AW. Effect of solid material on the blow-off limit of CH4/air flames in a micro combustor with a plate flame holder and preheating channels. Energy Convers Manag 2015;101:552–60.

[37] Wan JL, Fan AW, Yao H. Effect of the length of a plate flame holder on flame blowout limit in a micro-combustor with preheating channels. Combust Flame 2016;170:53–62.

[38] Beskok A, Karniadakis G. A model for flows in channels, pipes, and ducts at micro and nano scales. Microscale Thermophys Eng 1999;3:43–77.

[39] Fluent 14.0. Canonsburg, PA: User's Guide; 2011.

[40] Kee RJ, Grcar JF, Smooke MD, Miller JA. Sandia National Laboratories Report, SAND85-8240. 1994.

[41] Bilger RW, Starner SH. On reduced mechanisms for methane air combustion in nonpremixed flames. Combust Flame 1990;80:135–49.

[42] Holman JP. Heat transfer. 9th ed. New York: McGraw-Hill; 2002.

[43] Ma Q, Fang R, Xiang L. Handbook of thermo-physical properties (in chinese). Bejing: China Agricultural Machinery Press; 1986.

[44] Wan JL, Zhao H. Blow-off mechanism of a holder-stabilized laminar premixed flame in a preheated mesoscale combustor. Combust Flame 2020;220:358–67.

[45] Fan AW, Wan JL, Liu Y, Pi BM, Yao H, Maruta K, et al. The effect of the blockage ratio on the blow-off limit of a hydrogen/air flame in a planar micro-combustor with a bluff body. Int J Hydrogen Energy 2013;38:11438–45.

[46] Law CK. Combustion physics. Cambridge: Cambridge University press; 2006.

[47] Wan JL, Cheng X. Numerical investigation of the local extinction and re-ignition mechanisms of premixed flame in a micro combustor with a flame holder and preheating channels. Fuel 2020;264:116837.

[48] Kedia KS, Ghoniem AF. The blow-off mechanism of a bluff-body stabilized laminar premixed flame. Combust Flame 2015;162:1304–15.

[49] Jiménez C, Michaels D, Ghoniem AF. Ultra-lean hydrogen-enriched oscillating flames behind a heat conducting bluff-body: anomalous and normal blow–off. Proc Combust Inst 2019;37:1843–50.

[50] Wan JL, Zhao H. Effect of thermal condition of solid wall on the stabilization of a preheated and holder-stabilized laminar premixed flame. At Energ 2020;200:117548.

[51] Barlow RS, Dunn MJ, Sweeney MS, Hochgreb S. Effects of preferential transport in turbulent bluff-body-stabilized lean premixed CH4/air flames. Combust Flame 2012;159:2563–75.

[52] Kedia KS, Ghoniem AF. The anchoring mechanism of a bluff-body stabilized laminar premixed flame. Combust Flame 2014;161:2327–39.

[53] Jiménez C, Michaels D, Ghoniem AF. Stabilization of ultra-lean hydrogen enriched inverted flames behind a bluff–body and the phenomenon of anomalous blow–off. Combust Flame 2018;191:86–98.